Direct Synthesis of Graphdiyne Nanowalls on Arbitrary Substrates and Its Application for Photoelectrochemical Water Splitting Cell

Xin Gao, Jian Li, Ran Du, Jingyuan Zhou, Mao-Yong Huang, Rong Liu, Jie Li, Ziqian Xie, Li-Zhu Wu, Zhongfan Liu,* and Jin Zhang**

Graphdiyne (GDY), a novel 2D carbon allotrope, has been predicted to exhibit extraordinary properties.[1–3] Its uniformly distributed pores, unique sp–sp^2 carbon atoms, and high carrier mobility promise its diverse applications such as lithium-ion batteries,[4–6] catalysis,[7,8] and solar cells.[9,10] Fabricating GDY-based functional devices frequently calls for the transfer deposition of structure-controlled GDY onto specific substrates. However, limitations exist for the transfer process, which need to be overcome before the realization of practical applications. For example, it is difficult to keep the GDY structures stable during complicated transfer processes, especially for carefully designed GDY structures.[11] Moreover, the target substrates usually have variable dimensions and surface morphologies, making the coverage of GDY on a substrate with microstructures and contact at the interface between the transferred GDY and substrate hard to control. Thus, direct growth of GDY with different well-defined structures and distinct properties on target substrates is highly desirable, giving the capability of maintaining good quality and special structures of GDY. By carefully combining structure-tailored GDY with specific substrates, a wealth of functional materials having remarkable performance would be acquired.

Several attempts to prepare GDY with controlled architectures have been reported. Compared with dry chemistry such as the chemical vapor deposition (CVD) process,[12–14] a wet chemical route provides a more cost-effective and scalable approach to prepare large-area GDY suitable for practical applications. The synthesis of GDY by a wet chemical method was first realized on copper foil via a Glaser coupling reaction,[15] where the copper foil served as both reservoir of catalysts and planar template catering for the conformal growth of 2D GDY sheets. Following this pioneering work, our group further demonstrated that the morphology of GDY could be finely controlled by using a modified Hay–Glaser coupling reaction under optimized reaction conditions. Unique vertically grown GDY nanowalls were fabricated on either copper foils[11,16] or foams.[17] In all the above works, the selection of the substrate was limited by the catalyst, thus the growth of GDY was confined to copper substrates. One work[18] reported GDY nanotube arrays fabricated on an aluminum oxide template, the bottom of which was fixed to a copper foil as the catalyst source. However, up to now, the growth of structure-controlled GDY was only realized on selected or specially fabricated substrates, which is not desirable for the in situ fabrication of GDY-based functional devices, impeding the development of further applications of GDY. On this basis, we envision that the active catalysts can be effectively transferred to arbitrary substrates by rational design, realizing the in situ growth of GDY on target substrates, which will provide a wealth of potential applications for GDY.

Herein, we developed a new route to synthesize structure-controlled GDY by employing a copper envelope catalysis strategy, which is a general and simple method for the fabrication of GDY nanowalls on arbitrary substrates. In this method, the target substrates were put into a copper foil envelope borrowed from the CVD growth of graphene,[19] which ensures that sufficient concentrations of catalyst can diffuse into the interface between the target substrate and solution to induce the in situ growth of GDY. In detail, in alkaline solution, copper is believed to transform to a copper-pyridine complex,[15,20] acting as a "running catalyst" for acetylenic coupling reaction. Driven by concentration gradients, the "running catalyst" diffused from the copper envelope to the surface of target substrates where the acetylenic coupling reaction took place. The as-prepared copper envelope not only served as the catalyst reservoir but also was used as a container for arbitrary substrates, paving the way forward for the realization of GDY growth on target substrates with versatile chemical compositions and dimensions. Through this method, structure-controlled GDY grown on either 1D (Si nanowires), 2D (Au, Ni, W foils, and quartz), and even 3D substrates (stainless steel mesh and

X. Gao, R. Du, J. Zhou, R. Liu, J. Li, Z. Xie, Prof. Z. Liu, Prof. J. Zhang
Center for Nanochemistry
Beijing Science and Engineering Center for Nanocarbons
Beijing National Laboratory for Molecular Sciences (BNLMS)
College of Chemistry and Molecular Engineering
Peking University
Beijing 100871, China
E-mail: zfliu@pku.edu.cn; jinzhang@pku.edu.cn

J. Li, M.-Y. Huang, Prof. L.-Z. Wu
Key Laboratory of Photochemical Conversion and Optoelectronic Materials
Technical Institute of Physics and Chemistry
the Chinese Academy of Sciences
Beijing 100190, P. R. China
E-mail: lzwu@mail.ipc.ac.cn

J. Zhou, R. Liu
Academy for Advanced Interdisciplinary Studies
Peking University
Beijing 100871, P. R. China

DOI: 10.1002/adma.201605308

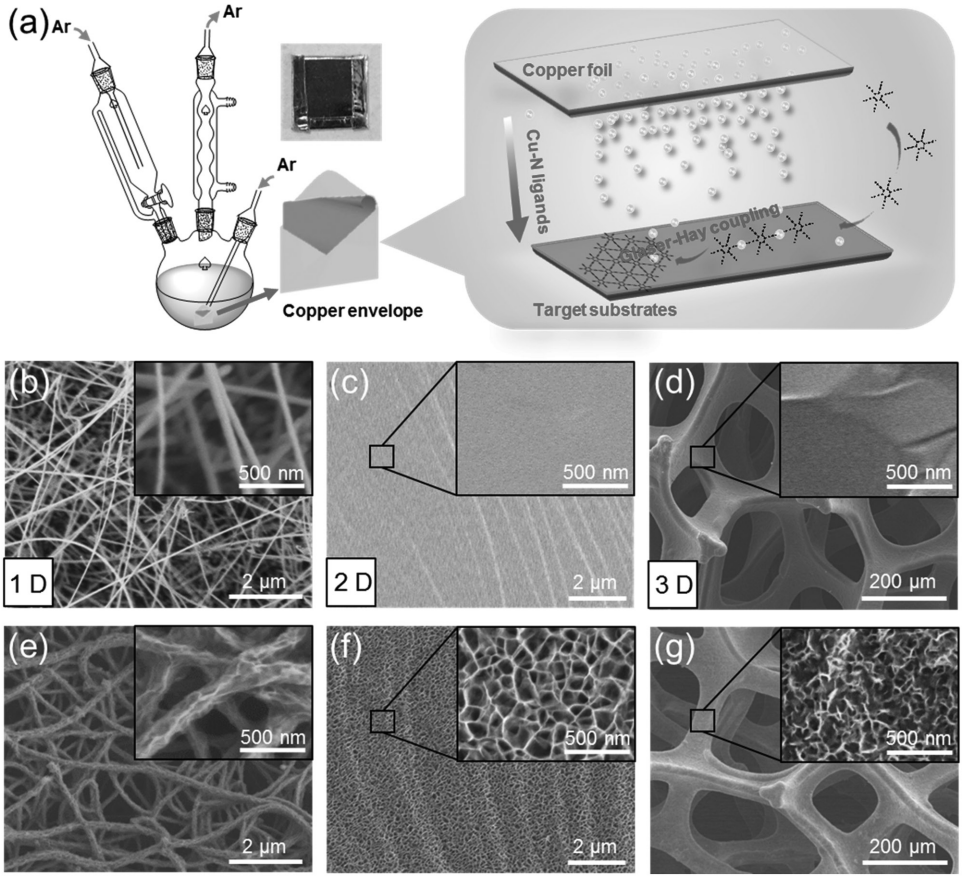

Figure 1. Synthesis of GDY nanowalls on arbitrary substrates via copper envelope catalysis. a) Schematic illustration of the experimental setup. SEM images of typical substrates before and after growth of GDY nanowalls: b,e) on 1D silicon nanowires, c,f) on 2D Au foil, and d,g) on 3D GF grown on Ni foam; closeup images are in the corresponding insets.

graphene foam (GF)) was realized. To demonstrate the value of this method, we introduce GDY into the photoelectrochemical water splitting cell, which could achieve the efficient conversion and storage of solar energy.[21–23] A GDY/$BiVO_4$ photoanode was fabricated by the direct synthesis of GDY nanowalls on $BiVO_4$ electrodes. $BiVO_4$ is regarded as one of the most promising photoanode materials[24–26] but suffers from high electron–hole recombination rate and poor water oxidation kinetics. Several attempts have been reported about establishing feasible pathways to address these problems,[27–29] but remains a challenge. In the new system, structure-controlled GDY can extract the photogenerated holes to participate in water oxidation efficiently, realizing significantly improved photoelectrochemical activity and stability compared to bare $BiVO_4$ electrodes.

The process and proposed mechanism used to synthesize GDY nanowalls on arbitrary substrates is depicted in **Figure 1**a. First, the target substrates were put onto the surface of pretreated copper foil, then a copper envelope was formed by bending the pretreated copper foil and crimping the three remaining sides, in which the target substrates were close enough to the copper foil for the growth of GDY (Figure 1a, inset). The target substrates wrapped in the copper envelope were immersed in a mixed solution of *N*,*N*,*N*′,*N*′-tetramethylethylenediamine (TMEDA), pyridine, and acetone. In the above alkaline solution, copper is easy to transfer to Cu ions with the presence of catalytic amount of base (pyridine and TMEDA). The coordination of TMEDA to Cu ions formed the Cu-N ligand composites, which act as a "running catalyst" for an acetylenic coupling reaction. The "running catalyst" can diffuse from the copper envelope to target substrates driven by a concentration gradient. Meanwhile, an acetone solution of hexaethynylbenzene (HEB) was added dropwise, serving as the precursor for the synthesis of GDY. After heating the mixture under an argon atmosphere at 50 °C for 12 h, GDY had been synthesized on the target substrates where the acetylenic coupling reaction took place at the interface between the target substrate and solution. Further details of the synthesis experiments are described in the Experimental Section and in the Supporting Information.

Using this method, well-defined GDY microstructures were fabricated on different dimensional substrates including 1D nanowires, 2D foils, and 3D foams or meshes. As shown in Figure 1b,e, GDY nanowalls were successfully fabricated on silicon nanowires. Figure 1b is a scanning electron microscopy (SEM) image of as-grown silicon nanowires on Si/SiO_2 substrate, with diameters of 20–50 nanometers and lengths of several tens of micrometer, showing good uniformity and wire-like morphology. A copper envelope containing silicon nanowires was inserted into our reactor, and after GDY was synthesized using copper envelope catalysis, the surface of the

silicon nanowires was entirely covered with nanowalls, showing increased diameters of 100–130 nm (Figure 1e and Figure S1, Supporting Information). GDY was also grown on both conducting (Au, Ni, W foils) and insulating (SiO_2) 2D substrates, and on 3D stainless steel meshes and graphene foams. Closeup images of Au foil in Figure 1c,f show that the synthesis of GDY resulted in ordered porous nanostructures uniformly covering the surface of Au foil, with an average pore size of 150 nm. Figure 1d,g shows porous nanostructures uniformly covering the entire interconnected 3D scaffolds of GF after GDY was synthesized. The details of GDY grown on other substrates are described in Figure S2 (Supporting Information).

In addition, the structure and elementary composition of GDY synthesized by using the copper envelope catalysis strategy were studied systematically with transmission electron microscopy (TEM), energy dispersive X-ray spectroscopy (EDS), X-ray photoelectron spectroscopy (XPS), and Raman spectroscopy. **Figure 2**a displays the TEM image of as-prepared GDY on Au foil, which indicates that the GDY nanowalls are continuous. The thickness of GDY nanowalls is about 180 nm (Figure 2a, inset). A magnified TEM image was used to characterize each "wall" sheet (Figure 2b), which verified the sheet to be a flat and uniform film with a smooth surface. High-resolution TEM (HRTEM) characterization reveals the layer-to-layer distance of GDY sheets is 0.365 nm, which is larger than that of graphene (0.335 nm), consistent with previous reports.[30] The TEM EDS spectrum indicates that the GDY nanowalls are mainly composed of elemental carbon (Figure 2d). Figure 2c presents a high resolution asymmetric C 1s XPS spectrum of GDY. The C 1s peak can be deconvoluted into four subpeaks at 284.5, 285.3, 286.6, and 288.0 eV, corresponding to C−C (sp^2), C−C (sp), C−O and C=O, respectively.[31] The small amounts of oxygen-containing groups may come from oxidation of some terminal alkyne.

Raman spectroscopy is regarded as a powerful tool to monitor the existence of carbon–carbon triple bonds. Therefore, the bond structure of as-prepared samples on different substrates (Au, Ni, SiO_2, W, GF) was further examined by the Raman spectroscopy (Figure 2f and Figure S3, Supporting Information). As a result, four prominent peaks around 1381.8 , 1568.9, 1933.5, and 2177.8 cm^{-1} appeared, which is consistent with previously reported values. In particular, the peak at 1381.8 cm^{-1} corresponds to the breathing vibration of sp^2 carbon domains in aromatic rings (D band). The peak at 1568.9 cm^{-1} results from the first-order scattering of the E_{2g} mode for in-phase stretching vibration of sp^2 carbon lattice in aromatic rings (G band).[32] The peak at 2177.8 cm^{-1} can be attributed to the vibration of conjugated diyne links, indicating a successful coupling reaction.[33,34]

In this way, by elaborately combining structure-tailored GDY and specific substrates, a range of functional materials with remarkable performance can be obtained. As an example, $BiVO_4$ is regarded as one of the most promising photoanode materials. However, high electron–hole recombination rate and poor water oxidation kinetics of $BiVO_4$ photoanodes result in its poor oxygen evolution reaction (OER) activity and stability in photoelectrochemical water splitting applications. As shown below, direct synthesis of GDY nanowalls on $BiVO_4$ electrodes can improve the performance of $BiVO_4$ electrodes dramatically.

A porous $BiVO_4$ electrode was first synthesized on a fluorine doped tin oxide (FTO) substrate according to the reported route.[35] (Details are presented in the Experimental Section and the Supporting Information.) Then, a photoelectrochemical cell (PEC) based on the GDY/$BiVO_4$ composite electrode was fabricated by direct synthesis of GDY on the $BiVO_4$ electrode using the copper envelope catalysis strategy. The morphology and microstructure of $BiVO_4$ and GDY/$BiVO_4$ composite photoanodes were characterized by SEM and TEM. As shown

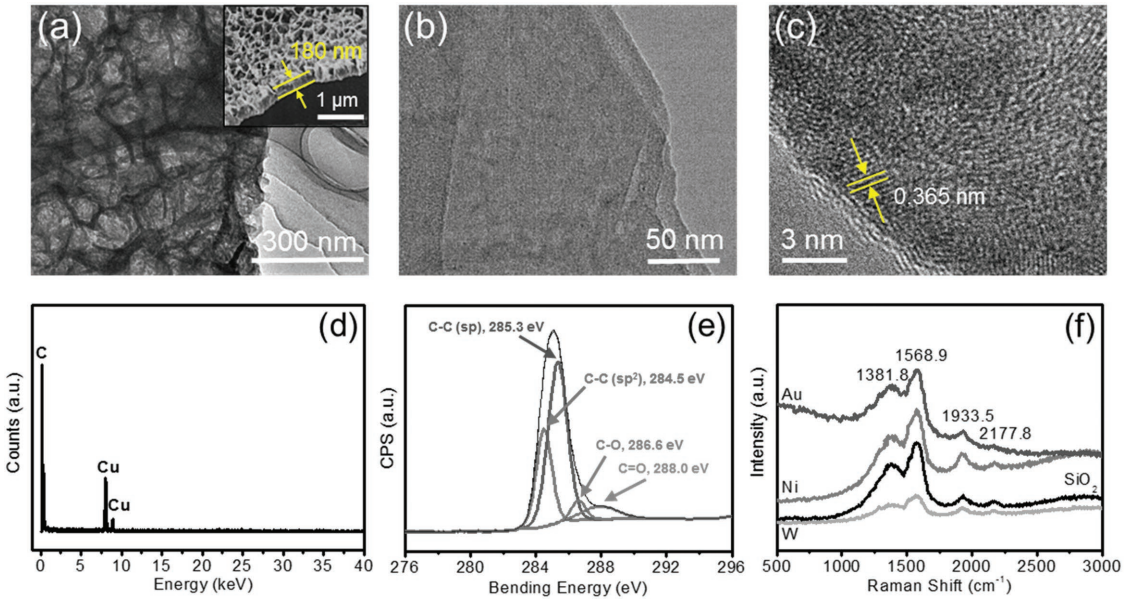

Figure 2. Characterization of as-prepared GDY nanowalls on various substrates. a,b) TEM images of as-prepared GDY nanowalls on Au foil. The inset of (a) is a cross-sectional view SEM image of the GDY nanowalls on Au foil. c) HRTEM image of as-prepared sample on Au foil. d) EDS spectrum of GDY nanowalls on copper grid. e) High-resolution core level XPS spectrum of C 1s. f) Typical Raman spectra of GDY nanowalls on different substrates.

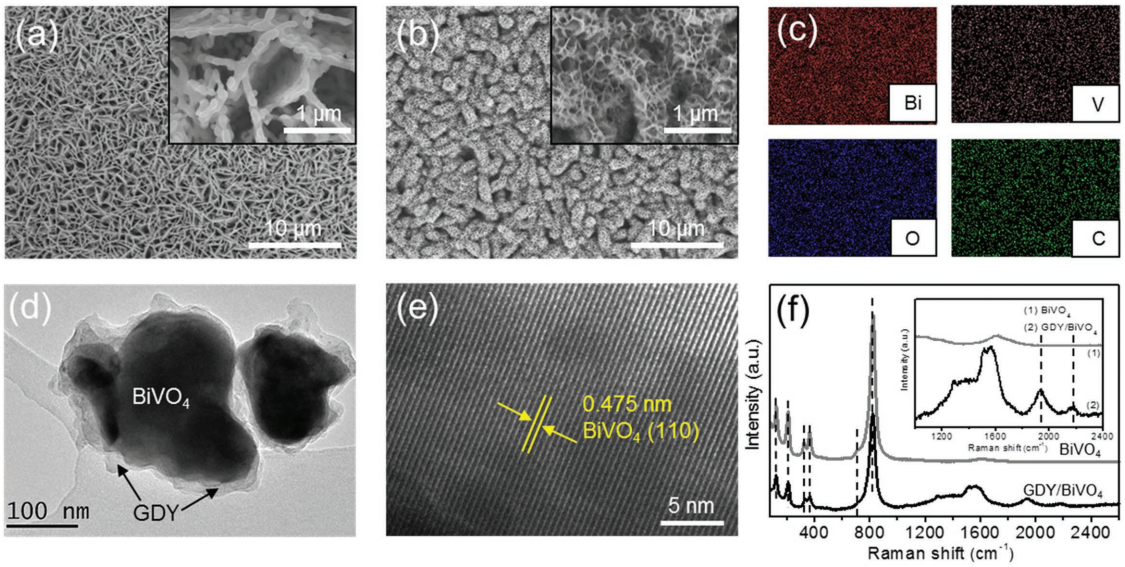

Figure 3. GDY nanowalls synthesized on $BiVO_4$ electrodes for photoelectrochemical cell applications. SEM images of a) $BiVO_4$ and b) the as-prepared GDY/$BiVO_4$. c) Elemental mapping of bismuth, vanadium, oxygen, and carbon by EDS. d) TEM image of GDY/$BiVO_4$. e) HRTEM image of the GDY/$BiVO_4$ recorded from a $BiVO_4$ nanosheet. f) Typical Raman spectra of as-prepared $BiVO_4$ (red) and GDY/$BiVO_4$ (black).

in **Figure 3**a, $BiVO_4$ shows an appearance of interconnected and aligned nanosheets, which are composed of numerous nanoparticles, forming a 3D microstructures on FTO substrate. After an acetylenic coupling reaction of HEB by using copper envelope catalysis, the surface of $BiVO_4$ was covered with 3D honeycomb-like GDY (Figure 3b). The corresponding elemental mapping from EDS of the GDY/$BiVO_4$ nanocomposites shows the presence of four elements (Bi, V, O, and C) in the composite, which is consistent with the XPS result (Figure S4, Supporting Information), indicating that C uniformly covered the surface of $BiVO_4$ (Figure 3c). A TEM image was used to further characterize the interface and the structure of GDY/$BiVO_4$. Figure 3d reveals that the $BiVO_4$ nanoparticles were embedded in the GDY matrix, indicating the sufficient contact and efficient interfacial interaction between GDY and $BiVO_4$. The HRTEM image (Figure 3e) taken from GDY/$BiVO_4$ shows a lattice fringe spacing of 0.475 nm, matching well with the (110) lattice plane of monoclinic $BiVO_4$.[36] The layer-to-layer distance of GDY sheets and the lattice fringe spacing of $BiVO_4$ around the interface of the GDY/$BiVO_4$ were shown in Figure S5 (Supporting Information). In addition, the XRD (X-ray diffraction) pattern of bare $BiVO_4$ on FTO could be indexed to the highly crystallized monoclinic $BiVO_4$ phase (JCPDS No. 14-0688) (Figure S6, Supporting Information). It is noteworthy that after coating GDY, the composites show coincident XRD patterns to the as-prepared $BiVO_4$, indicating that the process of forming GDY did not destroy the highly crystalline structure of $BiVO_4$ (Figure S6, Supporting Information).

Meanwhile, the typical Raman spectra of the as-prepared electrodes are presented in Figure 3f, showing peaks at 124.6, 209.5, 325.0, 365.9, 709.1, and 825.4 cm^{-1} for bare $BiVO_4$, in agreement with the previous reports.[37] The introduction of GDY could be further evidenced from the inset of Figure 3f. Compared with bare $BiVO_4$ electrodes, four prominent peaks around 1381.8, 1568.7, 1933.8, and 2177.7 cm^{-1} appeared, which are consistent with the previously reported results of GDY.[11] The UV–vis absorption behaviors of our as-prepared photoanodes were also investigated (Figure S7, Supporting Information). The absorption edge of $BiVO_4$ is at 520 nm. The bandgap of the $BiVO_4$ was estimated to be about 2.4 eV, which is close to the reported result of the monoclinic phase.[38]

The photoelectrochemical performance of the as-prepared electrodes was tested directly in a water splitting setup. A schematic illustration of the integrated photoanode and a possible mechanism for the improvement in photoelectrochemical water splitting performance are shown in **Figure 4**a. In contrast to the negligible current in the dark, both of the two samples exhibited obvious photocurrent under illumination from a 100 mW cm^{-2} Xe lamp, shown in Figure 4b. The onset potential of GDY/$BiVO_4$ photoanode catholically shifts from ≈0.6 to ≈0.4 V (vs. RHE, reversible hydrogen electrode) compared to the bare $BiVO_4$ photoanode. Meanwhile, the photocurrent density of the GDY-coated $BiVO_4$ photoanode was significantly higher than that of bare $BiVO_4$ photoanode at the potential of 0.4–1.4 V. A photocurrent density of about 1.32 mA cm^{-2} was obtained at the potential of 1.23 V versus RHE, which was nearly twice as high as that of $BiVO_4$ photoanode at the same potential. Moreover, after the addition of Co-Pi cocatalyst, the photoelectrochemical performance was further improved, with a photocurrent density of ≈2.03 mA cm^{-2} at 1.23 V versus RHE (Figure S8, Supporting Information). Further enhanced photoelectrochemical performance could be anticipated by tuning the compositions and structure of oxygen evolution cocatalysts. It has been reported that the accumulation of photoinduced holes by reason of poor water oxidation kinetics and charge transfer may bring about serious photocorrosion to the $BiVO_4$ electrode.[39] To verify the improved PEC stability of the composite photoanode against anodic photocorrosion, we investigated the *J*–*t* curves with long time illumination, shown in Figure 4c. The GDY-coated $BiVO_4$ film mainly maintained the original structure (Figure S9,

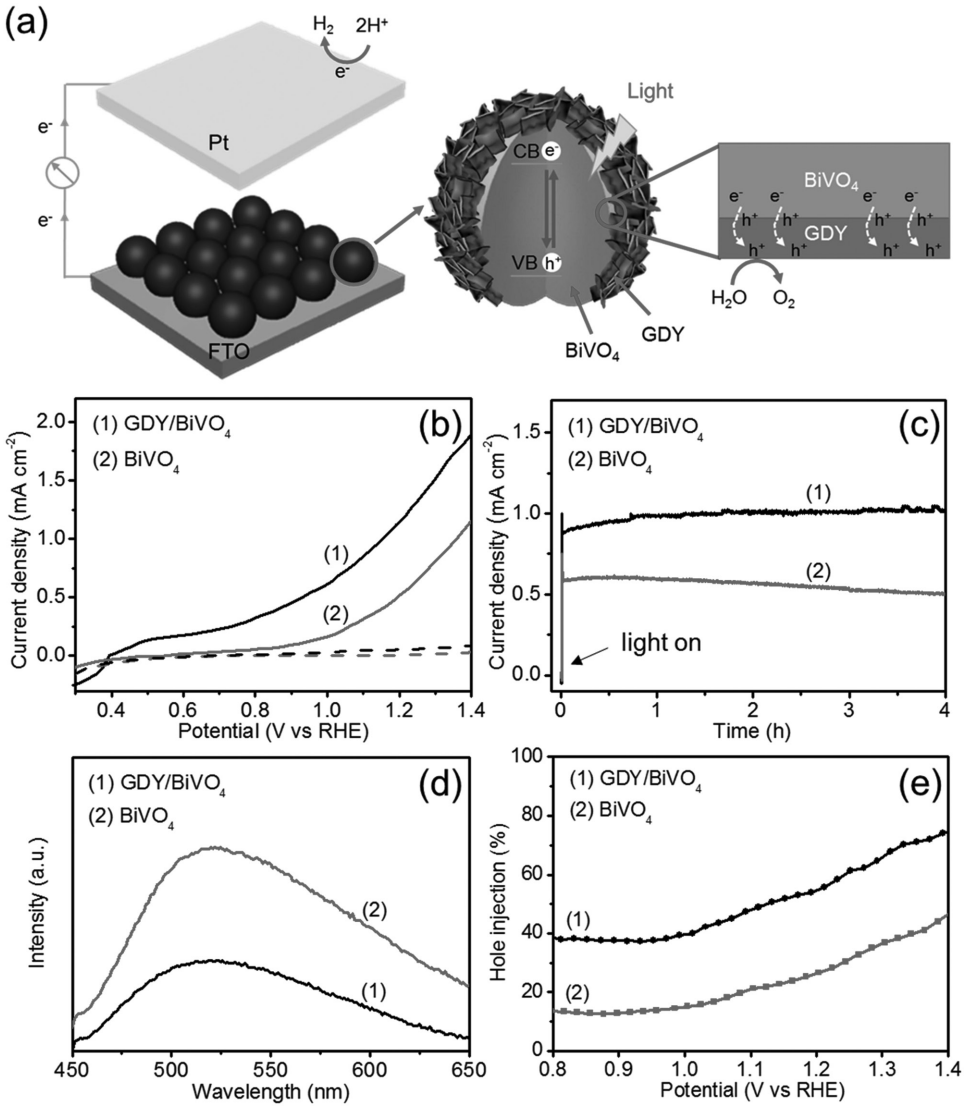

Figure 4. Photoelectrochemical performance of as-prepared samples. a) Schematic illustration of GDY/$BiVO_4$ photoanodes in a PEC setup and the migration of the photogenerated excitons at the interface. b) Current–voltage curves of $BiVO_4$ and GDY/$BiVO_4$ photoanodes under Xe lamp illumination (solid line) and in the dark (dashed line). c) *J–t* curves of $BiVO_4$ and GDY/$BiVO_4$ photoanodes in a 4 h test. d) Photoluminescence curves of $BiVO_4$ and GDY/$BiVO_4$ films. e) Hole injection yield of $BiVO_4$ and GDY/$BiVO_4$ photoanodes.

Supporting Information) and the photoelectrochemical activity with little change during a 4 h test, while a rapid decline in photocurrent (more than 20%) of bare $BiVO_4$ electrode was observed, indicating that GDY could significantly improve the stability of $BiVO_4$ electrode by rapidly extracting the photogenerated holes so that they are used for water oxidation rather than oxidizing $BiVO_4$ itself. Apart from the photocurrent performance, it is necessary to investigate in detail the behavior of hydrogen and oxygen evolution. Figure S10 (Supporting Information) presents the time courses of hydrogen and oxygen evolution by GDY/$BiVO_4$ photoanode at 1.23 V versus RHE. The faradaic efficiency can be calculated to be 85% during a 4 h test and the molar ratio of hydrogen and oxygen are nearly consistent with the stoichiometric ratio 2:1, an indication of successful splitting of water.

In order to further investigate the mechanism of enhanced photoelectrochemical behavior of GDY-coated $BiVO_4$ electrode, we carried out photoluminescence (PL) spectroscopy (Figure 4d) and electrochemical impedance spectroscopy (EIS) (Figure S11, Supporting Information) of the samples. After the deposition of GDY on the surface of $BiVO_4$, significant photoluminescence quenching effects could be detected, suggesting that the energy-wasting and undesirable charge recombination process was significantly suppressed due to the efficient extraction of photogenerated carriers from $BiVO_4$ by the GDY layer. Moreover, a much smaller EIS semicircle was observed from the sample of GDY/$BiVO_4$, implying a decreased charge transfer resistance and reduced recombination rate. To quantify the influence of GDY on the improvement of charge separation, the hole injection yield for water oxidation was determined by previous method[40] and shown in Figure 4e. The hole injection yield can be expressed simply by the following equation

$$P_{\text{charge injection}} = J_{\text{photocurrent}(H_2O)}/J_{\text{photocurrent}(H_2O_2)} \quad (1)$$

where $P_{\text{charge injection}}$ represents the injection yield of photogenerated holes to electrolyte for water oxidation reaction; $J_{\text{photocurrent}(H_2O)}$ and $J_{\text{photocurrent}(H_2O_2)}$ represent the photocurrent from H_2O oxidation and H_2O_2 oxidation, respectively, which could be extracted from Figures S12 and S13 (Supporting Information). More details of the equation are shown in the Supporting Information. The results showed that the hole injection yield could reach 60% at 1.23 V versus RHE, higher than that of bare $BiVO_4$ (less than 30%), demonstrating that GDY could efficiently accelerate the charge separation process. Based on the above discussion, we can establish the probable mechanism for the enhanced photoelectrochemical behavior of GDY-coated $BiVO_4$ electrode. First, $BiVO_4$ is excited under visible light and generates holes and electrons in the valance band and conduction band. The addition of GDY on the surface of $BiVO_4$ could extract the photogenerated holes efficiently due to its high hole mobility and unique vertically grown nanowalls structure, which allows most of the photogenerated holes to reach the electrode/electrolyte interface and participate in the water oxidation reaction, thus improving the efficiency of photoelectrochemical water splitting.

In summary, we have presented a simple design to generate GDY nanowalls on arbitrary substrates via Glaser–Hay coupling by using copper envelope catalysis. Copper-pyridine complex, which acts as a "running catalyst" for acetylenic coupling reaction, can diffuse from the copper envelope to target substrates. By Glaser–Hay coupling reaction of HEB monomers, GDY can be synthesized on target substrates including 1D (Si nanowires Au, Ni, and W foils), 2D (Au, Ni, W foils, and quartz), and 3D substrates (stainless steel meshes and graphene foam). In particular, a composite GDY/$BiVO_4$ photoanode was fabricated by direct synthesis of GDY nanowalls on a $BiVO_4$ electrode. Owing to the high hole mobility in GDY, a considerable enhancement of the photoelectrochemical behavior of $BiVO_4$ has been demonstrated through photoelectrochemical water splitting with the GDY coating. A photocurrent density of 1.32 mA cm^{-2} was obtained at a potential of 1.23 V versus RHE, which was nearly two times as high as that of bare $BiVO_4$, along with a more negative water oxidation onset potential. The improved OER activity is attributed to the formation of well-defined GDY/$BiVO_4$ interfaces. The GDY/$BiVO_4$ system is but one example of combining the unique properties of GDY with those of target substrates; there is great potential to make other combinations to improve the performance in various fields such as energy storage and photoelectric device.

Experimental Section

Preparation of $BiVO_4$: Nanoporous $BiVO_4$ electrodes were prepared by electrochemically depositing BiOI film onto fluorine-doped tin oxide (FTO) and applying a dimethylsulfoxide solution of vanadyl acetylacetonate [VO(acac)$_2$] onto the surface and heating in air in a muffle furnace at 450 °C for 1 h, converting BiOI to $BiVO_4$ (see the Supporting Information for more details).

Preparation of GDY/$BiVO_4$: The GDY/$BiVO_4$ electrode was prepared by employing a copper envelope catalysis strategy. As-prepared GDY-grown electrode was washed with heated acetone, *N*,*N*-dimethylformamide, pyridine, sequentially, to remove monomers, oligomers, and catalyst, then dried under a flow of nitrogen. This protocol creates the GDY/$BiVO_4$ photoanode (see the Supporting Information for more details).

Supporting Information

Supporting Information is available from the Wiley Online Library or from the author.

Acknowledgements

X.G. and J.L. contributed equally to this work. This work was supported by the Ministry of Science and Technology of China (2016YFA0200101, 2016YFA0200104 and 2014CB239402), the National Natural Science Foundation of China (grant 51432002, 21129001, 21233001), and CAS Interdisciplinary Innovation Team.

Received: October 1, 2016
Revised: October 24, 2016
Published online: December 23, 2016

[1] L. D. Pan, L. Z. Zhang, B. Q. Song, S. X. Du, H. J. Gao, *Appl. Phys. Lett.* **2011**, *98*, 173102.
[2] M. Long, L. Tang, D. Wang, Y. Li, Z. Shuai, *ACS Nano* **2011**, *5*, 2593.
[3] Y. Li, L. Xu, H. Liu, *Chem. Soc. Rev.* **2014**, *43*, 2572.
[4] C. Sun, D. J. Searles, *J. Phys. Chem. C* **2012**, *116*, 26222.
[5] S. Zhang, H. Liu, C. Huang, G. Cui, Y. Li, *Chem. Commun.* **2015**, *51*, 1834.
[6] S. Zhang, H. Du, J. He, C. Huang, H. Liu, G. Cui, Y. Li, *ACS Appl. Mat. Interfaces* **2016**, *8*, 8467.
[7] H. Qi, P. Yu, Y. Wang, G. Han, H. Liu, Y. Yi, Y. Li, L. Mao, *J. Am. Chem. Soc.* **2015**, *137*, 5260.
[8] S. Wang, L. Yi, J. E. Halpert, X. Lai, Y. Liu, H. Cao, R. Yu, D. Wang, Y. Li, *Small* **2012**, *8*, 265.
[9] Z. Jin, M. Yuan, H. Li, H. Yang, Q. Zhou, H. Liu, X. Lan, M. Liu, J. Wang, E. H. Sargent, Y. Li, *Adv. Funct. Mater.* **2016**, *26*, 5284.
[10] J. Xiao, J. Shi, H. Liu, Y. Xu, S. Lv, Y. Luo, D. Li, Q. Meng, Y. Li, *Adv. Energy Mater.* **2015**, *5*, 1401943.
[11] J. Zhou, X. Gao, R. Liu, Z. Xie, J. Yang, S. Zhang, G. Zhang, H. Liu, Y. Li, J. Zhang, Z. Liu, *J. Am. Chem. Soc.* **2015**, *137*, 7596.
[12] X. Qian, Z. Ning, Y. Li, H. Liu, C. Ouyang, Q. Chen, *Dalton Trans.* **2012**, *41*, 730.
[13] X. Qian, H. Liu, C. Huang, S. Chen, L. Zhang, Y. Li, J. Wang, *Sci. Rep.* **2015**, *5*, 7756.
[14] Y. Q. Zhang, N. Kepcija, M. Kleinschrodt, K. Diller, S. Fischer, A. C. Papageorgiou, F. Allegretti, J. Bjork, S. Klyatskaya, F. Klappenberger, M. Ruben, J. V. Barth, *Nat. Commun.* **2012**, *3*, 1286.
[15] G. Li, Y. Li, H. Liu, Y. Guo, D. Zhu, *Chem. Commun.* **2010**, *46*, 3256.
[16] J. Li, X. Gao, B. Liu, Q. Feng, X. B. Li, M. Y. Huang, Z. Liu, J. Zhang, C. H. Tung, L. Z. Wu, *J. Am. Chem. Soc.* **2016**, *138*, 3954.
[17] X. Gao, J. Zhou, R. Du, Z. Xie, S. Deng, R. Liu, Z. Liu, J. Zhang, *Adv. Mater.* **2016**, *28*, 168.
[18] G. Li, Y. Li, X. Qian, H. Liu, H. Lin, N. Chen, Y. Li, *J. Phys. Chem. C* **2011**, *115*, 2611.
[19] W. Fang, A. L. Hsu, Y. Song, A. G. Birdwell, M. Amani, M. Dubey, M. S. Dresselhaus, T. Palacios, J. Kong, *ACS Nano* **2014**, *8*, 6491.
[20] N. Hebert, A. Beck, R. B. Lennox, G. Just, *J. Org. Chem.* **1992**, *57*, 1777.

[21] J. Zhang, W. Zhao, Y. Xu, H. Xu, B. Zhang, *Int. J. Hydrogen Energy* **2014**, *39*, 702.
[22] Y. Hou, F. Zuo, A. P. Dagg, J. Liu, P. Feng, *Adv. Mater.* **2014**, *26*, 5043.
[23] Y. Huang, Y. Liu, D. Zhou, Y. Xin, B. Zhang, *J. Mater. Chem. A* **2016**, *4*, 13626.
[24] W. He, R. Wang, L. Zhang, J. Zhu, X. Xiang, F. Li, *J. Mater. Chem. A* **2015**, *3*, 17977.
[25] H. M. Chen, C. K. Chen, R. S. Liu, L. Zhang, J. Zhang, D. P. Wilkinson, *Chem. Soc. Rev.* **2012**, *41*, 5654.
[26] R. Li, F. Zhang, D. Wang, J. Yang, M. Li, J. Zhu, X. Zhou, H. Han, C. Li, *Nat. Commun.* **2013**, *4*, 1432.
[27] M. Ma, J. K. Kim, K. Zhang, X. Shi, S. J. Kim, J. H. Moon, J. H. Park, *Chem. Mater.* **2014**, *26*, 5592.
[28] S. J. A. Moniz, J. Zhu, J. Tang, *Adv. Energy Mater.* **2014**, *4*, 1301590.
[29] B. Liu, J. Li, H.-L. Wu, W.-Q. Liu, X. Jiang, Z.-J. Li, B. Chen, C.-H. Tung, L.-Z. Wu, *ACS Appl. Mater. Interfaces* **2016**, *8*, 18577.
[30] C. Huang, S. Zhang, H. Liu, Y. Li, G. Cui, Y. Li, *Nano Energy* **2015**, *11*, 481.
[31] H. Estrade-Szwarckopf, *Carbon* **2004**, *42*, 1713.
[32] A. C. Ferrari, J. C. Meyer, V. Scardaci, C. Casiraghi, M. Lazzeri, F. Mauri, S. Piscanec, D. Jiang, K. S. Novoselov, S. Roth, A. K. Geim, *Phys. Rev. Lett.* **2006**, *97*, 187401.
[33] J. Y. Wang, S. Q. Zhang, J. Y. Zhou, R. Liu, R. Du, H. Xu, Z. F. Liu, J. Zhang, Z. R. Liu, *Phys. Chem. Chem. Phys.* **2014**, *16*, 11303.
[34] S. Zhang, J. Wang, Z. Li, R. Zhao, L. Tong, Z. Liu, J. Zhang, Z. Liu, *J. Phys. Chem. C* **2016**, *120*, 10605.
[35] T. W. Kim, K.-S. Choi, *Science* **2014**, *343*, 990.
[36] C. Yin, S. Zhu, Z. Chen, W. Zhang, J. Gu, D. Zhang, *J. Mater. Chem. A* **2013**, *1*, 8367.
[37] J. Yu, A. Kudo, *Adv. Funct. Mater.* **2006**, *16*, 2163.
[38] Y. Wang, W. Wang, H. Mao, Y. Lu, J. Lu, J. Huang, Z. Ye, B. Lu, *ACS Appl. Mater. Interfaces* **2014**, *6*, 12698.
[39] K. J. McDonald, K.-S. Choi, *Energy Environ. Sci.* **2012**, *5*, 8553.
[40] E. S. Kim, H. J. Kang, G. Magesh, J. Y. Kim, J. W. Jang, J. S. Lee, *ACS Appl. Mater. Interfaces* **2014**, *6*, 17762.